Heat and Mass Transfer 37 (2001) 67–76 © Springer-Verlag 2001

Heat and mass transfer analogy for condensation of humid air in a vertical channel

G. Desrayaud, G. Lauriat

Abstract This study examines energy transport associated with liquid film condensation in natural convection flows driven by differences in density due to temperature and concentration gradients. The condensation problem is based on the thin-film assumptions. The most common compositional gradient, which is encountered in humid air at ambient temperature is considered. A steady laminar Boussinesq flow of an ideal gas–vapor mixture is studied for the case of a vertical parallel plate channel. New correlations for the latent and sensible Nusselt numbers are established, and the heat and mass transfer analogy between the sensible Nusselt number and Sherwood number is demonstrated.

List of symbols

A	channel aspect ratio, $A = H/b$
b	channel width, m
C_p	specific heat capacity at constant pressure, $J \cdot kg^{-1}\ K^{-1}$
D	binary diffusion coefficient, $m \cdot s^{-2}$
g	gravitational acceleration, $m \cdot s^{-2}$
G	reduced flow rate
h	specific enthalpy, $J \cdot kg^{-1}$
h_{fg}	latent enthalpy, $J \cdot kg^{-1}$
H	channel length, m
$\mathbf{j}$	diffusional mass flux vector, $kg \cdot m^{-2}\ s^{-1}$
k	thermal conductivity, $W \cdot m^{-1} \cdot K^{-1}$
Le	Lewis number, $Le = \alpha/D$
$\dot{m}$	condensation mass flux, $kg \cdot m^{-2}\ s^{-1}$
M	molecular weight, $kg \cdot mol^{-1}$
$\dot{M}$	dimensionless condensation mass flow rate
N	buoyancy parameter, $Ra_M/(Le\ Ra_T)$
Nu_s	sensible Nusselt number
Nu_ℓ	latent Nusselt number
p	pressure, Pa
p_{ps}	partial pressure of water vapor at saturation condition, Pa
P_m	dimensionless dynamic pressure, $P_m = b^2 p_m/\rho_0 \alpha^2$
Pr	Prandtl number, $Pr = \nu/\alpha$
$\mathbf{q}$	heat flux vector, $W \cdot m^{-2}$
Ra_M	mass Rayleigh number, $Ra_M = g\beta_M(w_0 - w_s)b^3/\nu D$
Ra_T	thermal Rayleigh number, $Ra_T = g\beta_T(T_0 - T_w)b^3/\nu\alpha$
Ra_M^*	channel mass Rayleigh number, Ra_M/A
Ra_T^*	channel thermal Rayleigh number, Ra_T/A
RA	combined Rayleigh number, $RA = Ra_T(1 + N/Le^{0.5})$
RA^*	channel combined Rayleigh number, $RA^* = Ra_T^*(1 + N/Le^{0.5})$
T	temperature, K
U	dimensionless longitudinal velocity, $U = ub/\alpha$
V	dimensionless transverse velocity, $V = vb/\alpha$
$\mathbf{V}$	dimensionless velocity vector
w	mass fraction of water vapor
W	reduced mass fraction of water vapor, $W = (w - w_s)/\Delta w$
X	dimensionless longitudinal coordinate, $X = x/b$
Y	dimensionless transverse coordinate, $Y = y/b$
α	thermal diffusivity, $m^2 \cdot s^{-1}$
β_M	solutal coefficient of volumetric expansion, $\beta_M = M_a/M_v - 1$
β_T	thermal coefficient of volumetric expansion, $\beta_T = 1/T_r$, K^{-1}
γ	dimensionless parameter, $\gamma = (C_{pv} - C_{pa})\Delta w/C_{pr}$
Γ	ratio of latent heat flux to sensible heat flux, $\Gamma = h_{fg}/C_{pr}\Delta T$
θ	reduced temperature, $\theta = (T - T_w)/\Delta T$
Θ_r	temperature ratio, $\Theta_r = \Delta T/T_r$
ρ	density, $kg \cdot m^{-3}$
ν	kinematic viscosity, $m^2 \cdot s^{-1}$
ϕ_0	relative humidity of air at ambient condition
ΔT	reference temperature difference, $\Delta T = T_0 - T_w$
Δw	reference mass fraction difference, $\Delta w = w_0 - w_s$

Subscripts

0	at ambient condition
a	of air
r	at reference condition, evaluated at $T_r = (T_0 + T_w)/2$ and $w_r = (w_0 + w_s)/2$
s	at saturation condition
v	of water vapor
w	at wall

Received on 15 November 1999

G. Desrayaud (✉)
INSSET, Université de Picardie
48 rue Raspail, BP 422
02109 Saint-Quentin Cedex, France

G. Lauriat
Université de Marne-la-Vallée
Bât. Lavoisier, Champs-sur-Marne
77454 Marne-la-Vallée Cédex 02, France

This work was supported by research grants from the IDRIS-Computer Center (French National Institute for Advances in Scientific Computations, Grants no 980715). One of the authors (G.D.) wishes to acknowledge the financial support of this work by the Picardie region (Pôle Modélisation).

1 Introduction

Natural convection heat transfer in vertical open channel flows induced by the buoyancy of thermal diffusion alone has been the subject of numerous studies for various geometric configurations since it concerns a number of applications, ranging from the cooling of electronic equipment to the heating of buildings. The resurgence of interest in this problem comes from the low cost of such devices, which do not introduce electromagnetic or acoustic noises, although their applicability is restricted to low power density. In natural convective cooling or heating systems with humid air as the working fluid, undesirable effect of condensation may appear.

Natural convection processes involving combined heat and mass gradients of binary mixture has been widely studied. Correlations for the sensible heat transfer by natural convection were first obtained numerically and experimentally in vertical cavities with uniform temperature and uniform concentration at the vertical walls [1–3]. Nelson and Wood [4] have derived a correlation for developing natural convection heat transfer between vertical parallel plates. The work of Nelson and Wood was based on the integral analysis of Somers [5] for natural convection along a vertical flat plate. Recently, Lee [6] performed a numerical investigation of combined heat and mass transfer in open vertical parallel plates with unheated entry and unheated exit for various thermal and concentration boundary conditions. He demonstrated that the presence of unheated entry or exit severely affects the heat and mass transfer rates. Nevertheless, the solutions approach asymptotically the closed form solutions for the fully developed flow. Lee [6] also presented mean Nusselt number and Sherwood number correlations in the developing and single plate regimes. Others studies have been carried out to investigate the effect of latent heat transfer during evaporation or condensation phenomena from a wetted surface to a binary mixture with a single condensable vapor. Detailed analyses of the heat and mass transfer processes between a binary mixture and a liquid film are complex owing to the coupling at the film–gas interface. Thus, by assuming that the liquid film is extremely thin, transport phenomena in the film can be replaced by approximate boundary conditions for the gas flow, whereas conservation equations of boundary-layer type are numerically solved for the gas flow. This type of analysis was conducted in the case of evaporation in vertical channels for laminar forced convection [7] and for natural convection [8]. Heat and mass transfer with consideration of transport processes in the liquid film was numerically investigated by Yan and Lin [9] and Yan [10]. They demonstrated that the assumption of a thin liquid film thickness is a limiting condition, which is only valid for systems in which the liquid mass flow rate is very small.

The above review reveals that most of the previous analytical and numerical works were based on the two-dimensional parabolic forms of the governing equations, which result from simplifications of boundary-layer type. Recently, studies were conducted by using the full elliptic form of the momentum and energy equations for thermal convection in a vertical plate channel [11, 12]. It has been shown that the two formulations yield results in quite good agreement provided that the channel Rayleigh number is high enough. Nevertheless, boundary-layer approximations cannot predict flow reversals.

This work is primarily focused on heat and mass transfer for a gas stream inside a vertical cooled channel in which phase change may occur, a particular attention being paid to the phase change of water vapor at the walls. Under the assumption of thin liquid film, heat and mass transport within the film can be approximated by appropriate boundary conditions for the gas flow at the walls. Condensation of humid air is investigated and comparisons between sensible and latent heat fluxes due to phase change are discussed. Correlations for the sensible mean Nusselt and Sherwood numbers are given also. Relationships between the mean parameters are determined and the heat and mass transfer analogy (Lewis assumption) is shown to be valid for the set of parameters considered in the present study.

2 Analysis

2.1 Model equations

In this section, the question of the problem formulation is considered first. The dimensionless field equations and boundary conditions are written for a two-dimensional steady flow of humid air in a vertical isothermal channel of aspect ratio A (length/width), as illustrated in Fig. 1.

Humid air with a relative humidity ϕ_0 enters the vertical channel with a flat velocity profile, u_0, uniform temperature and concentration profiles, T_0 and w_0 respectively. The binary mixture is drawn into the channel by the combined buoyancy forces due to the non-uniformity in the temperature and concentration of water vapor fields. The channel walls are maintained at constant temperature, T_w. When the temperature of the channel walls is below the dew-point temperature of humid air, part of vapor condenses and forms a thin liquid film on the walls. The treatment of the complex flow motion within the liquid film and at the interface is circumvented by

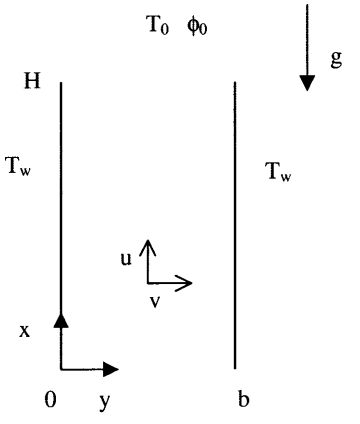

Fig. 1. Schematic configuration of the physical model

assuming an extremely thin liquid film. Also, the density variation is assumed to be important only in the buoyancy force term (Boussinesq approximation), and may be modeled as a linear function of temperature and mass fraction; thus, we are considering small temperature variations and low concentrations of water vapor in the mixture. This results in:

$$\frac{\rho_0 - \rho}{\rho} = \beta_T(T - T_0) + \beta_M(w - w_0)$$

The dimensionless forms of the continuity and momentum equations for the mixture may be written as:

$$\nabla \cdot \mathbf{V} = 0 \tag{1}$$

$$\nabla(\mathbf{V} \cdot \mathbf{V}) = -\nabla P_m + \mathrm{Pr}\nabla^2\mathbf{V} + \left(\mathrm{Ra_T Pr}\theta + \frac{\mathrm{Ra_M Pr}}{\mathrm{Le}} W\right)\mathbf{k} \tag{2}$$

The dimensionless conservation equation for energy reads:

$$\nabla \cdot (\theta\mathbf{V}) = \nabla^2\theta + \frac{1}{\mathrm{Le}}\nabla \cdot [\gamma(\theta - 0.5)\nabla W] \tag{3}$$

If condensation takes place only at the boundaries, the conservation of vapor in the flow field requires:

$$\nabla \cdot (W\mathbf{V}) = \frac{1}{\mathrm{Le}}\nabla^2 W \tag{4}$$

The last term on the RHS of Eq. (3) represents the energy transport through the interdiffusion of the species, air and water vapor. Equation (4) is based on a constant diffusivity assumption.

Both dependent and independent variables introduced in the above equations have been non-dimensionalized as follows:

$$X = x/b, \quad Y = y/b, \quad U = ub/\alpha, \quad V = vb/\alpha,$$
$$P_m = b^2 p_m/\rho_0\alpha^2, \quad \gamma = (C_{pv} - C_{pa})\Delta w/C_{pr},$$
$$\theta = (T - T_w)/\Delta T, \quad W = (w - w_s)/\Delta w$$

The thermophysical properties of the mixture are taken constant and evaluated at the reference temperature and concentration, i.e. $T_r = (T_0 + T_w)/2$ and $w_r = (w_0 + w_s)/2$. The Prandtl and Lewis numbers are respectively $\mathrm{Pr} = \nu/\alpha$ and $\mathrm{Le} = \alpha/D$. For a binary mixture such as air–water vapor, the typical values are Pr = 0.71 and Le = 0.86.

Since the molecular weight of water vapor is smaller than that of dry air, the buoyancy force due to mass transfer and the buoyancy force of thermal diffusion act downwards in the case of condensation. Thus, the flow in the channel is always downwards. Thermal and mass Rayleigh numbers have then always positive values and are defined as

$$\mathrm{Ra_T} = g\beta_T(T_0 - T_w)b^3/\nu\alpha$$
$$\mathrm{Ra_M} = g\beta_M(w_0 - w_s)b^3/\nu D$$

Instead of using the mass Rayleigh number, a combination of these two Rayleigh numbers can be introduced, the buoyancy parameter which is

$$N = \frac{\beta_M\Delta w}{\beta_T\Delta T} = \frac{\mathrm{Ra_M}}{\mathrm{Le\ Ra_T}}$$

By assuming that the humid air–liquid film interface is in thermodynamic equilibrium and that humid air is an ideal gas mixture of dry air and water vapor, the interfacial mass fraction of water vapor is related to the partial pressure of the water vapor at saturation condition, p_{ps}, at the wall temperature through the equation:

$$w_s = 0.622\ p_{ps}/(p - 0.378\ p_{ps}) \tag{5}$$

Although Eq. (5) indicates that the saturated mass fraction of water vapor varies with the pressure, w_s was used as a reference scale in the nondimensionalizing procedure owing to the very small change in the pressure along the channel height. This was numerically confirmed in [7, 8] for evaporation of humid air in laminar natural and mixed convection flows in vertical channels.

When neglecting species interdiffusion, Dufour and Soret effects, the dimensional heat and species fluxes at the walls are respectively:

$$q = q_s + q_\ell = -k\partial T/\partial y + \dot{m}h_{fg} \tag{6a}$$

$$j_v = -\rho D\partial w/\partial y \tag{6b}$$

The second term on the right-hand side of Eq. (6a) represents the contribution of the condensation of water vapor.

Since the liquid film at the wall surface is assumed to be of negligible thickness, it can be considered as a boundary condition for heat and mass transfer with the film at the wall temperature. The condensation rate of water vapor at the walls is then evaluated by

$$\dot{m} = \rho v_w = \rho\frac{D}{1 - w_s}\frac{\partial w}{\partial y}\bigg|_w \tag{7}$$

The dimensionless velocity of the mixture at the interface and the boundary conditions at the walls are thus:

$$V_w = \pm\left(\frac{\Delta w}{\mathrm{Le}(1 - w_s)}\frac{\partial W}{\partial Y}\right)_w \quad U = 0, \quad \theta = 0, \text{ and}$$
$$W = 0 \quad \text{at } Y = 0, 1 \tag{8}$$

In the momentum equation (2), the pressure defect has been introduced to model the acceleration of the stagnant ambient fluid through the channel inlet. Special considerations have been brought for modeling the boundary conditions both at the inlet (use of the Bernoulli equation for the pressure defect) and at the outlet sections in order to investigate possible flow reversals. At the channel exit, the flow is assumed to become a free jet, which expands in a local hydrostatic pressure field at the exit elevation. Therefore, pressure boundary conditions are imposed at inlet and outlet. With the imposed pressure boundary condition at the inlet section, the average longitudinal velocity, U_0, is an outcome of the solution and it is assumed to be uniform. It has been shown indeed that the velocity profile at the inlet section tends to be flat for moderate values of the channel thermal Rayleigh number, $\mathrm{Ra_T^*}$ [13]. Therefore, the following conditions were imposed at the ends of the channel,

at the inlet,

$$X = A \quad U = U_0 \quad V = 0 \quad \theta = 1 \quad W = 1 \quad P_m = -U_0^2/2 \tag{9a}$$

at the outlet,

$$X = 0 \quad \frac{\partial U}{\partial X} = \frac{\partial V}{\partial X} = 0 \quad \frac{\partial \theta}{\partial X} = 0 \quad \frac{\partial W}{\partial X} = 0 \quad P_m = 0 \tag{9b}$$

If flow reversal occurs at the outlet section, the boundary conditions for temperature and mass fraction are then taken as the ambient conditions on the part of the section where $U > 0$.

According to the above assumptions, Eqs. (6)–(7), the local Nusselt number at the wall can be expressed as:

$$\mathrm{Nu} = \frac{h(x)b}{k} = \frac{q(x)}{(k\Delta T/b)} = -\partial\theta/\partial Y + \Gamma V_w \tag{10a}$$

The second term on the right hand side of Eq. (10a) represents the latent heat transfer. Here, $\Gamma = h_{fg}/C_{pr}\Delta T$ characterizes the ratio of the latent heat flux of water vapor to the reference for the sensible heat flux of the binary mixture, V_w is the suction at the walls defined by Eq. (8). It is worth noting that it is not a constant for various ambient or wall conditions, since it depends on the temperature difference.

The mean Nusselt number is obtained as,

$$\overline{\mathrm{Nu}} = \frac{\bar{h}b}{k} = -\frac{\overline{\partial\theta}}{\partial Y} + \frac{\Gamma\dot{M}}{A} = \overline{\mathrm{Nu}}_s + \overline{\mathrm{Nu}}_\ell \quad \text{with}$$

$$\dot{M} = \int_0^A V_w \, dX = \int_0^A \left(\frac{\dot{m}b}{\rho\alpha}\right) dX \tag{10b}$$

The mean Sherwood number at the walls is,

$$\overline{\mathrm{Sh}} = \overline{h_M}b/D = -\overline{\partial W}/\partial Y \tag{11}$$

One of the constraints to be satisfied for the solution of a steady channel flow is the overall mass balance for humid air at every longitudinal location. It reads in dimensional form:

$$\rho u_0 b = \int_0^b \rho u(x) dy + 2\int_H^x \dot{m} \, dx \tag{12a}$$

This overall mass balance is used in the solution procedure to check the convergence of the numerical solutions. The dimensionless inlet mass flow rate is defined as $G = |U_0|$. This leads to

$$U_0 = \int_0^1 U|_{X=0} \, dY + 2\int_0^A V_w \, dX = \int_0^1 U|_{X=0} \, dY - 2\dot{M} \tag{12b}$$

Combining Eqs. (8), (10) and (11), a relationship between the mean parameters of the problem, $\overline{\mathrm{Nu}}_\ell$, $\overline{\mathrm{Sh}}$ and $\dot{M}$, is obtained as:

$$\overline{\mathrm{Nu}}_\ell = \Gamma\frac{\dot{M}}{A} = \frac{\Gamma\,\Delta w}{\mathrm{Le}(1-w_s)}\,\frac{\overline{\partial W}}{\partial Y} = \frac{\Gamma\,\Delta w}{\mathrm{Le}(1-w_s)}\,\overline{\mathrm{Sh}} \tag{13}$$

Using the definitions of the buoyancy parameter, N, and of Γ, Eq. (13) can be rewritten and new relationships between the mean variables are thus obtained as:

$$\frac{\overline{\mathrm{Nu}}_\ell}{N\Gamma\Theta_r} = \frac{\dot{M}}{AN\Theta_r} = \left(\frac{1}{\beta_M}\right)\frac{\overline{\mathrm{Sh}}}{\mathrm{Le}(1-w_s)} \tag{14}$$

where $\Theta_r = \Delta T/T_r$ is the temperature ratio. This parameter will be used in what follows to properly correlate the latent Nusselt number.

3 Solution method

The governing equations were solved in primitive variables by using a control volume method and by employing the SIMPLER algorithm for the velocity-pressure coupling [14]. The momentum, energy and concentration equations were cast in transient form and the time-integration was performed by using an ADI scheme until a steady state was obtained. At high Rayleigh numbers, a streamline second-order upwinding was introduced to damp out spurious oscillations caused by the advection terms (QUICK scheme). Under-relaxation parameters were used for velocities to control the advancement of the solution field.

To check the adequacy of the numerical scheme employed for solving the full elliptic Navier–Stokes and energy equations, results for the case of natural convection flows induced by thermal buoyancy forces alone were compared with those of Naylor et al. [11]. A quite good agreement was found, as it is shown in Table 1. To gain confidence in the methodology used to study binary mixtures, the numerical code was then applied to double diffusion natural convection in a square cavity. The vertical walls are maintained at constant and uniform, but different temperatures and concentrations while the horizontal walls are adiabatic and impermeable. The results based on the present computational code were compared with those of Bennacer [15]. Table 2 shows that the

Table 1. Comparison of mean Nusselt number and mass flow rate in vertical isothermal channels

	$A = 5$, $\mathrm{Ra}_T^* = 1467$ Pr = 0.733		$A = 12$, $\mathrm{Ra}_T^* = 4667$ Pr = 0.7	
	$\overline{\mathrm{Nu}}$	G	$\overline{\mathrm{Nu}}$	G
Present results	3.75	69.59	4.96	289.63
Naylor et al. [11]	3.73	74.55	4.81	290.22
Correlation (15)	3.62	–	4.87	–

Table 2. Comparison of mean Nusselt and Sherwood numbers for various values of the buoyancy parameter, N, in a square enclosure. $Ra_T = 7 \times 10^3$, Pr = 7

		N	0.1	0.5	1	10
$\overline{Nu}$	Le = 1	Present results	2.08	2.31	2.54	4.38
		Bennacer [15]	2.06	2.29	2.52	4.36
	Le = 10	Present results	2.03	2.07	2.10	1.86
		Bennacer [15]	2.03	2.07	2.11	1.88
$\overline{Sh}$	Le = 1	Present results	2.08	2.31	2.54	4.38
		Bennacer [15]	2.06	2.29	2.52	4.36
	Le = 10	Present results	5.25	5.53	5.84	8.84
		Bennacer [15]	5.03	5.35	5.82	8.66

agreement in the mean Nusselt (respectively Sherwood) numbers at the vertical walls is within 1% (resp. 4%) for $Ra_T = 7 \times 10^3$, Pr = 7, and for various values of the Lewis number and of the buoyancy parameter, N. The values of the mean Nusselt and Sherwood numbers computed for Le = 1 are obviously identical.

In the present work, uniform mesh sizes were used for the x-direction while meshes were non-uniformly distributed in the y-direction, the grid being more dense near the walls of the channel. Tests with various grid sizes showed that a grid of 101×42 for the aspect ratio A = 10 was refined enough to model accurately the flow fields described in this study. For instance, for the case 7 (see Table 3) results with a grid of 151×52 showed that the relative differences in the mean sensible and latent Nusselt numbers, mean Sherwood number, inlet mass flow rate, and condensation mass flux were negligibly small (less than 0.5%). For aspect ratios of 15 and 20, 125×32 and 155×32 grid sizes were utilized.

4 Results and discussion

First, a brief review of natural convection in vertical channels induced by the buoyancy of thermal diffusion alone is presented. In his pioneering experimental work of natural convection in vertical heated channels, Elenbaas [16] showed that the Nusselt values are bounded over the complete range of flow development by the analytic relations for the fully developed limit and the isolated plate limit. This result has been proved for different thermal boundary conditions by Bar-Cohen and Rohsenow [17]. The correlation of the mean Nusselt number (based on the channel width) as a function of the channel thermal Rayleigh number for symmetric isothermal channel reads:

$$\overline{Nu} = \left[576/Ra_T^{*2} + 2.873/\sqrt{Ra_T^*}\right]^{-0.5} \qquad (15)$$

where $Ra_T^* = Ra_T/A$ is the channel thermal Rayleigh number.

The mean Nusselt numbers calculated with this correlation are reported in Table 1. The agreement with the present results is better than 2% for the highest value of the channel thermal Rayleigh number while it reaches 3.5% for the lowest value. However, discrepancies were found at values of the channel thermal Rayleigh number of the order of 10^2or less (fully developed flow) for which the fluid becomes heated by conduction far upstream from the channel inlet. Indeed, a heat conductive counter-flow preheats then the incoming air. At these low flow rates, the computational domain must be extended far away from the inlet section. In the present study, the channel Rayleigh number is assumed to be large enough so that the flow is in the developing flow regime or in the isolated plate regime.

The computational procedure was then applied to examine the effects of the condensation of a thin film of liquid water on heat transfer and on mass flow-rate of humid air flowing downward in channels of arbitrary aspect ratio. The ambient air–water vapor mixture, at a temperature greater than that of the walls, is drawn into the channel by the combined buoyancy forces of heat and mass transfer. Calculations were conducted to examine the importance of the latent heat flux released by condensation at the walls, which can affect the natural convection heat and mass transfer.

With a view to practical situations, most of the calculations were performed for the physical parameters reported in Table 3. The aspect ratio was varied with the channel height kept fixed for the first set (cases 1–5) while the channel width was unchanged for the second set (cases 1 and 6–9). Flows of unsaturated humid air enter the channel at relative humidity, ϕ_0(ranging from 50–90%), and at atmospheric pressure. The wall temperature is kept constant at $T_w = 5\,^\circ$C. The channel thermal and mass Rayleigh numbers reported in Table 3 were calculated for an ambient temperature, $T_0 = 25\,^\circ$C. The buoyancy parameter is almost constant for a given relative humidity, i.e. $N \approx 0.03$ for $\phi_0 = 50\%$ and $N \approx 0.1$ for $\phi_0 = 90\%$. For ambient situations like those considered in this study, the

Table 3. Values of parameters for various cases with $T_0 = 25\,^\circ$C and $T_w = 5\,^\circ$C ($\Delta T = 20\,^\circ$C). Pr = 0.71, Le = 0.86

Case	b (m)	H (m)	A	Ra_T^*	Ra_M^*	
					$\phi_0 = 50\%$	$\phi_0 = 90\%$
1	0.1	0.5	5	4.52×10^5	1.50×10^4	4.19×10^4
2	0.0625	0.5	8	6.91×10^4	2.29×10^3	6.40×10^3
3	0.05	0.5	10	2.83×10^4	9.37×10^2	2.62×10^3
4	0.025	0.5	20	1.77×10^3	5.86×10^1	1.63×10^2
5	0.02	0.5	25	7.24×10^2	2.40×10^1	6.66×10^1
6	0.1	0.8	8	2.82×10^5	9.38×10^3	2.62×10^4
7	0.1	1.0	10	2.26×10^5	7.50×10^3	2.10×10^4
8	0.1	1.5	15	1.50×10^5	5.00×10^3	1.40×10^4
9	0.1	2.0	20	1.13×10^5	3.75×10^3	1.05×10^4

mass transfer is mostly driven by temperature difference owing to the very dilute fraction of the water vapor in air. The dimensionless parameters being not independent, it has been found preferable to show in Table 3 the dimensional variables from which the dimensionless parameters were calculated.

The transverse profiles for dimensionless velocity, temperature and mass fraction at the mid-height of the channel are displayed in Fig. 2a–c for two values of the channel thermal Rayleigh number located at both ends of the range of Ra_T^* considered in the present study. The profiles of the longitudinal velocity-component (Fig. 2a) clearly demonstrate the change in the flow structure from the developing regime ($Ra_T^* = 724$) to the single-plate regime ($Ra_T^* = 4.52 \times 10^5$) for which two separate boundary layers develop. It is worth noting that the temperature and mass fraction profiles are almost parabolic for $Ra_T^* = 724$ although the flow field is developing. The transverse dimensionless mass fraction profiles plotted in Fig. 2c ($W = 0$ at the walls where condensation occurs) show that the temperature and mass fraction profiles (Fig. 2b, c) are very similar, the largest differences being at low values of the channel Rayleigh number. The explanation is that the Lewis number is close to unity for air–water vapor mixtures. Due to the very dilute fraction of water vapor in air at ambient temperature, the velocity and temperature profiles (2a, b) are almost identical to those found in a vertical channel without phase change.

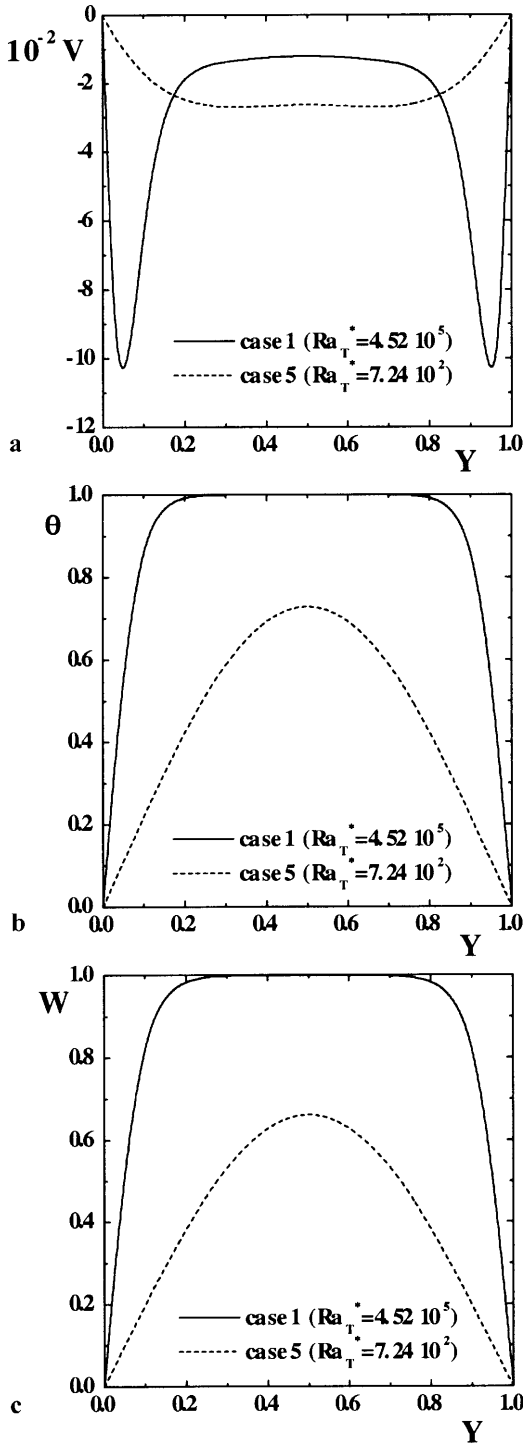

Fig. 2a–c. Transverse profiles of the longitudinal velocity **a**, temperature **b** and mass fraction **c** at $X = 0.5$ for the cases 1 and 5 from Table 3; $T_0 = 25\ ^\circ C$, $T_w = 5\ ^\circ C$, $\phi_0 = 50\%$

A brief summary of relevant studies for dilute binary mixtures in which the Soret (mass flux due to temperature gradient) and Dufour (energy flux due to concentration gradient) diffusion effects are neglected is given here. With regard to transport phenomena by natural convection on a vertical plate, the combined Rayleigh number, $RA = Ra_T(1 + N/Le^{0.5})$, has been introduced originally by Somers [5] in his integral analysis and by Gebhart et al. [18] to correlate the sensible Nusselt and Sherwood numbers for $Pr \approx 1$ and $Le \approx 1$ as

$$\begin{aligned} \overline{Nu}_s &= B\ Ra_T^{1/4}\left[1 + N/Le^{0.5}\right]^{1/4} = B\ RA^{1/4} \\ \overline{Sh} &= B\ Ra_M^{1/4}\left[1 + Le^{0.5}/N\right]^{1/4} = B\ Le^{3/8} RA^{1/4} \end{aligned} \tag{16}$$

where the characteristic length is the height of the plate and B is an independent coefficient.

The analogy between heat and mass transfer leads to

$$\frac{\overline{Sh}}{\overline{Nu}_s} = Le^{3/8} = Le^{0.375} \tag{17}$$

For an electrochemical system with $Pr \approx 7$ and $Sc \approx 2100$, Kamotani et al. [1] used the correlation suggested by Somers [5] which was established for thermosolutal convection along a vertical flat plate. The mean Sherwood number relation is

$$\overline{Sh} = 0.68\ Le^{3/8} RA^{1/4} \tag{18}$$

Kamotani et al. [1] experimentally confirmed the validity of this relation in the case of shallow enclosures with combined horizontal temperature and concentration gradients, and showed that it is better suited for cooperating solutal and thermal buoyancy forces ($N > 0$). For pure thermal convection, they observed indeed that the heat transfer rate approaches to that corresponding to a vertical plate if the Rayleigh number is high enough. Kamotani et al. [1] applied then the vertical plate correlation for combined thermal and solutal convection. The group $Ra_T^*(1 + N/Le^{0.5})$ was used later on by Nelson and Wood [4] for natural convection in a vertical channel by using the channel width as the characteristic length and the

channel thermal Rayleigh number. In what follows, this group will be denoted RA^* and named channel combined Rayleigh number.

$$\begin{aligned}\overline{Nu_s} &= 0.705\left[Ra_T^*\left(1+N/Le^{0.5}\right)\right]^{0.230} \\ &= 0.705 RA^{*0.230} \\ \overline{Sh} &= 0.559\left[Le^2 Ra_T^*\left(1+N/Le^{0.5}\right)\right]^{0.239} \\ &= 0.559 Le^{0.478} RA^{*0.239}\end{aligned} \tag{19}$$

Slightly different correlations were recently proposed by Lee [6] who used $Ra_T^*(1+N)$ as the main parameter. This dimensionless group comes from theoretical considerations relative of the fully developed regime and Lee extended its usefulness to the developing and single plate regimes. This gives for the mean sensible Nusselt and Sherwood correlations the following relationships,

$$\begin{aligned}\overline{Nu_s} &= \left\{\begin{matrix}0.842\\0.581\end{matrix}\right\}\left[Ra_T^*(1+N)\right]^{0.233} \\ \overline{Sh} &= \left\{\begin{matrix}0.906\\0.482\end{matrix}\right\}\left[LeRa_T^*(1+N)\right]^{0.233}\end{aligned} \tag{20}$$

In his study, Lee [6] gives upper and lower limits for the Nusselt and Sherwood correlations because the heated part of the channel can have an unheated entry or an unheated exit. For long enough unheated exit, the heat transfer can be increased by 50% due to the chimney effect. On the other hand, unheated entry causes a severe flow restriction. This is why their numerical results are found inside an envelope whose upper and lower limits are given by Lee. These limits are also given in brackets in Eqs. (20).

In the present study, correlations of the form of Eq. (16) were found. The $Ra^{1/4}$-dependence is well supported by the numerical calculations, not only for the isolated plate regime but also for the developing flow regime. This result is first illustrated in Fig. 3 where the sensible mean Nusselt numbers is reported as a function of the channel combined Rayleigh number, RA^*. Computations have been carried out for the parameters given in Table 3 (cross symbol) and also for two additional temperature differences: open circles for $\Delta T = 10\,^\circ C$ ($T_0 = 15\,^\circ C$, $T_w = 5\,^\circ C$) and open triangles for $\Delta T = 15\,^\circ C$ ($T_0 = 15\,^\circ C$, $T_w = 0\,^\circ C$). The present correlation for the mean sensible Nusselt number is

$$\overline{Nu_s} = 0.567\ RA^{*1/4} \tag{21}$$

The best fitted computations over the 81 numerical results gives an exponent value of 0.240 which is close to the boundary-layer characteristic value relevant to natural convection from a wetted isothermal flat plate, determined theoretically by Somers (i.e., 1/4). It is why the correlation (21) used this theoretical exponent value. In this case, the relative error is lower than 1% at $RA^* = 10^3$ and reaches 1.4% at $RA^* = 10^6$. As it can be seen, the correlation of Nelson and Wood (dot line) crosses over the full line representing Eq. (21), because the slope of their curve is lower (0.230 power). Nevertheless, the absolute value of the relative difference between the two sensible Nusselt correlations, Eqs. (19) and (21), is always lower than 5% whatever the combined channel Rayleigh number is. The

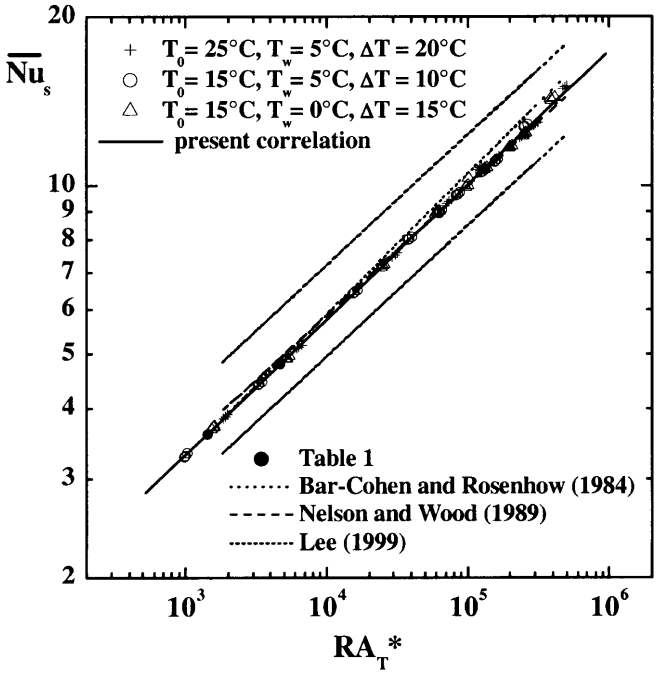

Fig. 3. Variation of the mean sensible Nusselt number versus combined channel Rayleigh number

Lewis number being close to one in the present study, the correlation (20) is presented in Fig. 3 versus RA^* to give valuable information. Our correlation is inside the envelope found by Lee [6]. The Bar-Cohen and Rohsenow correlation given by Eq. (15) is also drawn as a dashed line in Fig. 3 with $N = 0$. Our results reported in Table 1 for $N = 0$ are also displayed in Fig. 3 as filled black circles, and a rather good agreement can be seen between the correlation and these results. Although the values of the buoyancy parameters N are low in the present study, the curve for the correlation given by Eq. (21) is distinctly shifted downward.

The variation of the mean Sherwood number at the walls versus the combined channel Rayleigh number is shown in Fig. 4. It should be noticed first that, owing to the low values of the buoyancy parameter N, the mean Sherwood number is almost independent of the relative ambient humidity, ϕ_0, for a given temperature difference and a fixed wall temperature. According to the analytical finding of Somers [5], a 1/4 power was used to fit all of the 81 numerical results. The correlation is

$$\overline{Sh} = 0.563\ Le^{3/8} RA^{*1/4} \tag{22}$$

In the above equation, the $Le^{3/8}$ factor has been kept for convenience since the Lewis number is a constant in the present study. This correlation is drawn as a solid line in Fig. 4 together with the correlations of Kamotani et al. [1], Somers [5], Nelson and Wood [4] and Lee [6]. Surprisingly, although the present correlation for the sensible Nusselt number is very close to that of Nelson and Wood [4] as it is seen in Fig. 3, large differences are displayed between the results for the Sherwood number. The relative difference between the two curves, Eqs. (19) and (22), is close to 10% at $RA^* = 2000$ and reaches 14% at

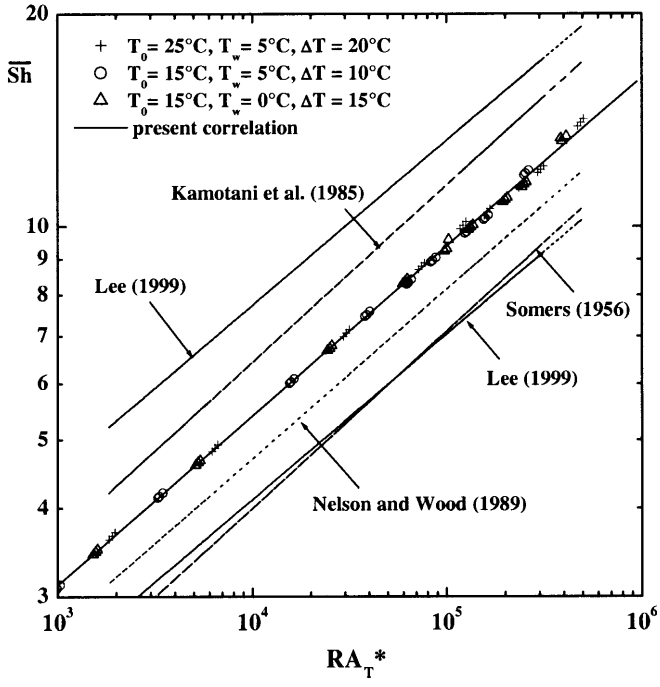

Fig. 4. Variation of the mean Sherwood number versus combined channel Rayleigh number

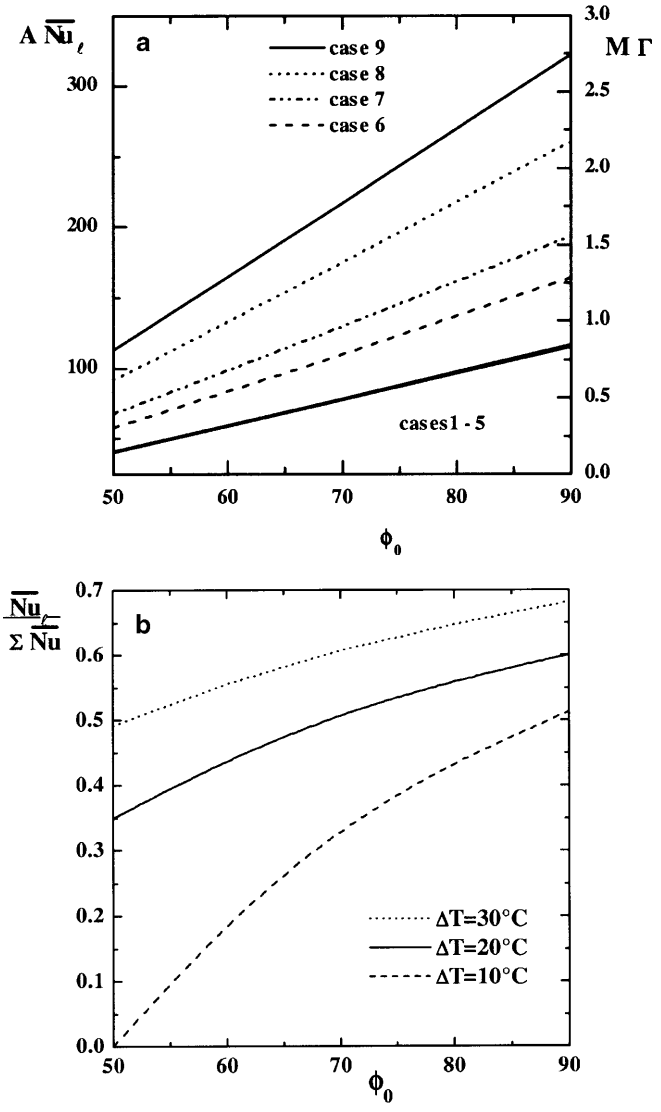

Fig. 5. **a** Variation of the mean latent Nusselt number and of the condensation flow rate as a function of the relative humidity; $T_0 = 25\ ^\circ C$, $T_w = 5\ ^\circ C$ ($\Delta T = 20\ ^\circ C$). **b** Variation of the fractions of the mean latent Nusselt number as a function of the relative humidity at the same wall temperature, $T_w = 5\ ^\circ C$ and for three different ambient temperatures

$RA^* = 5 \times 10^5$. In an attempt to elucidate this discrepancy, the ratio of the mean Sherwood number [Eq. (22)] to the sensible mean Nusselt number [Eq. (21)] was calculated to check the validity of the heat and mass transfer analogy. It is found that

$$\frac{\overline{Sh}}{\overline{Nu_s}} = 0.992\ Le^{3/8} = 0.937 \qquad (23)$$

This ratio being very close to unity, it is not surprising that the coefficients in Eqs. (21) and (22) do not differ much. The correlations (19) reported in [4] yield the following ratio

$$\frac{\overline{Sh}}{\overline{Nu_s}} = 0.793\ Le^{0.478} RA^{*0.009} = 0.738\ RA^{*0.009}$$

Therefore, the coefficient is quite far from unity. It should be noted that these correlations were obtained for a Prandtl number of 0.7, various Schmidt numbers between 0.2 and 5.0 and values of the buoyancy parameter in the range $-0.5 \leq N \leq 2$. Since it is well established that the results correlate better for cooperating buoyancy ($N > 0$) than for opposing buoyancy ($N < 0$) [1, 18], the discrepancy for $Le \approx 1$ between the Nelson and Wood correlation [4] and the present correlation for Sh is understandable.

Following Eq. (13) the variation of the mean latent Nusselt number based on the height of the channel ($A\ \overline{Nu}_\ell$) and the variation of the condensation mass flow rate ($\Gamma \dot{M}$) are shown in the same figure, Fig. 5a, as a function of the relative ambient humidity. Two series of computations were carried out: cases 1–5 are for the same channel height while cases 1 and 6–9 are for the same channel width (Table 3). All of the curves for the cases 1–5 are virtually indistinguishable. The explanation is that the changes in flow rate through the channel due to changes in width does not affect significantly the latent heat exchange. On the other hand, the mean latent Nusselt number and the slope of the curves increase as the channel height is increased. Such an heat transfer enhancement results from the increase in the chimney effect with H and, therefore, in the mean flow velocity.

The energy rejected by the humid air depends on two interdependent effects: the temperature difference between the air stream and the wall, producing sensible heat transfer, and the water vapor mass fraction difference, source of latent heat transfer. In order to illustrate the relative contribution of the sensible and latent heat exchanges, the ratio of the latent Nusselt number to the overall Nusselt number is presented in Fig. 5b in function

of the relative humidity at the inlet. It is noteworthy that all of the curves plotted in Fig. 5a for $\Delta T = 20\,^{\circ}\mathrm{C}$ collapse into one curve in Fig. 5b. This result can be demonstrated easily by using Eq. (13) to express the mean latent Nusselt number and by using the heat transfer analogy [Eq. (17) or (23)] to express the mean sensible Nusselt number. For a given mixture as it is the case here (i.e., constant Lewis number) the ratio of the latent Nusselt number to the overall Nusselt number depends only on the mass fraction of the water vapor (or on the relative humidity) at the inlet and on the temperature difference, ΔT, since the specific latent enthalpy is kept constant within the range of temperature considered. This is clearly seen in Fig. 5b where two other curves are presented for two ambient temperatures, $T_0 = 15$ and $35\,^{\circ}\mathrm{C}$, but at the same wall temperature, $T_w = 5\,^{\circ}\mathrm{C}$.

For the lowest temperature difference, which is also for the lowest ambient temperature ($T_0 = 15\,^{\circ}\mathrm{C}$), the dew point is at $4\,^{\circ}\mathrm{C}$ for $\phi_0 = 50\%$. This explains why there is no latent heat flux released in this case. For $T_0 = 25\,^{\circ}\mathrm{C}$ (respectively, $35\,^{\circ}\mathrm{C}$) condensation starts to occur at $\phi_0 = 30\%$ (resp. 20%); these values were determined by extrapolation. The specific latent enthalpy being very large, a small increase in the mass condensation flow rate at the walls resulting from an increase in ϕ_0 can cause a substantial enhancement of the latent heat exchange. This increase is all the more significant since the ambient temperature is low. For the two highest ambient temperatures, even if the latent heat ratio increases with the mass fraction, the increase is less pronounced than for $T_0 = 15\,^{\circ}\mathrm{C}$. Figure 5b reveals that the influence of latent heat exchange on the overall heat transfer is substantial, and that it is more important for high ambient temperature and/or mass fraction.

Finally, Fig. 6 presents the variation of the dimensionless group of the mean latent Nusselt number of Eq. (14) versus the combined channel Rayleigh number. Clearly, all the numerical predictions presented in Figs. 4 and 5 can be correlated as

$$\frac{\overline{\mathrm{Nu}}_\ell}{\Gamma N \Theta_r} = 1.021\ \mathrm{RA}^{*1/4} \qquad (24)$$

The knowledge of the temperature level T_r is thus required to correlate well the mean latent Nusselt number.

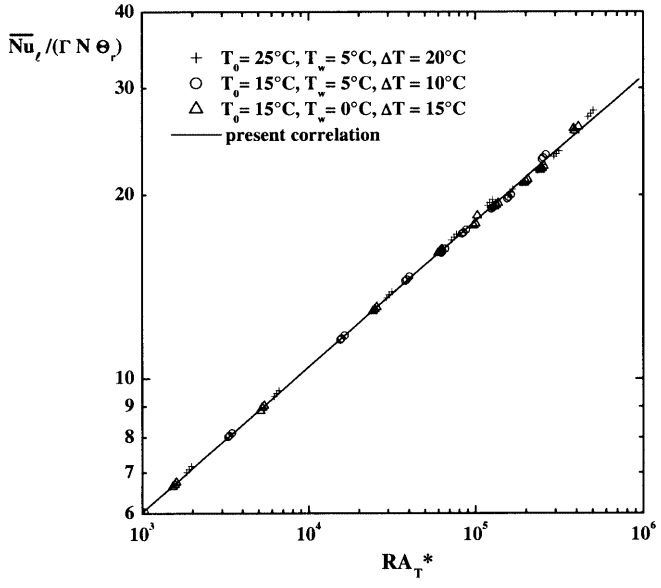

Fig. 6. Variation of the dimensionless group of the mean sensible Nusselt versus combined channel Rayleigh number

5 Conclusion

A numerical study has been carried out to investigate buoyancy induced heat and mass transfer of humid air flowing in a vertically heated channel. The air in the ambient is drawn into the channel by the coupling of thermal and solutal buoyancy forces.

Results have been presented for condensation of humid air at channel wall surfaces. The phase change problem is based on thin-film assumptions. Consequently, the induced air flow is in the downward direction since thermal buoyancy and solutal buoyancy act in the same direction. Owing to the low level of water vapor concentration, the flow and temperature fields are weakly affected by the buoyancy force of mass diffusion. It plays a negligible role in the determination of the flow regime: fully developed, developing or single-plate flow. On the opposite, the phase change at the wall surfaces may significantly contribute to the overall heat transfer, even if the condensation mass flow rate is small. Correlations between the main parameters were determined and the heat and mass transfer analogy was found to be still valid when condensation occurs.

References

1. **Kamotani Y; Wang LW; Ostrach S; Jiang HD** (1985) Experimental study of natural convection in shallow enclosures with horizontal temperature and concentration gradients. Int J Heat Mass Transfer 28: 165–173
2. **Trevisan OV; Bejan A** (1987) Combined heat and mass transfer by natural convection in a vertical enclosure. J Heat Transfer 109: 104–112
3. **Bennacer R; Gobin D** (1996) Cooperating thermosolutal convection in enclosures – 1. Scale analysis and mass transfer. Int J Heat Mass Transfer 39: 2671–2881
4. **Nelson DJ; Wood BD** (1989) Combined heat and mass transfer natural convection between vertical parallel plates. Int J Heat Mass Transfer 32: 1779–1787
5. **Somers EV** (1956) Theoretical considerations of combined thermal and mass transfer from a vertical flat plate. J Applied Mech 23: 295–301
6. **Lee KT** (1999) Natural convection heat and mass transfer in partially heated vertical parallel plates. Int J Heat Mass Transfer 42: 4417–4425
7. **Lin TF; Chang CJ; Yan WM** (1988) Analysis of combined buoyancy effects of thermal and mass diffusion on laminar forced convection heat transfer in a vertical tube. J Heat Transfer 110: 337–344
8. **Yan WM; Lin TF; Chang CJ** (1988) Combined heat and mass transfer in natural convection between vertical parallel plates, Warme- und Stoffubertr 23: 69–76
9. **Yan WM; Lin TF** (1990) Combined heat and mass transfer in natural convection between vertical parallel plates with film evaporation. Int J Heat Mass Transfer 33: 529–541
10. **Yan WM** (1992) Effects of film evaporation on laminar mixed convection heat and mass transfer in vertical channel. Int J Heat Mass Transfer 35: 3419–3429

11. **Naylor D; Floryan JM; Tarasuk JD** (1991) A numerical study of developing free convection between isothermal vertical plates. J Heat Transfer 113: 620–626
12. **Sefcik DM; Webb BW; Heaton HS** (1991) Analysis of natural convection in vertically-vented enclosures. Int J Heat Mass Transfer 34: 3037–3046
13. **Morrone B; Campo A; Manca O** (1997) Optimum plate separation in vertical parallel-plate channels for natural convection flows: incorporation of large spaces at the channel extremes. Int J Heat Mass Transfer 40: 993–1000
14. **Patankar SV** (1980) Numerical Heat Transfer and Fluid Flow. Washington, DC, Hemisphere Publishing
15. **Bennacer R** (1993) Convection naturelle thermosolutale: simulation numérique des transferts et des structures d'écoulement. thèse de doctorat, Paris VI
16. **Elenbaas W** (1942) Heat dissipation of parallel plates by free convection. Physica 9: 1–23
17. **Bar-Cohen A; Rohsenow WM** (1984) Thermally optimum spacing of vertical, natural convection cooled, parallel plates. J Heat Transfer 116: 116–123
18. **Gebhart B; Jaluria Y; Mahajan RL; Sammakia B** (1988) Buoyancy-induced Flows and Transport p 310 New York, Hemisphere Publishing Corp.